

The precession dynamo experiment at HZDR

Motivated by the idea of a precession-driven flow as energy source for the early geodynamo or the ancient lunar magnetic field, a large precession dynamo experiment is under development at HZDR.

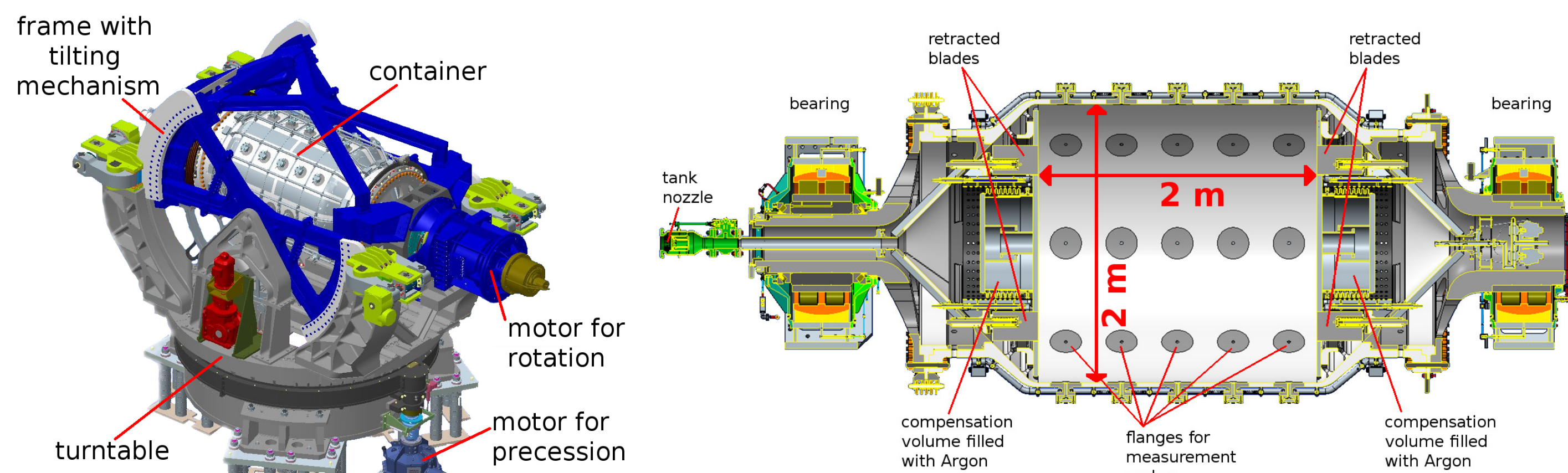


Fig. 1: Sketch of the facility (left) and the container (right). The cylinder has radius $R=1$ m and height $H=2$ m. The tilt between rotation axis and precession axis can be varied from 45° to 90° .

rotation rate	precession rate	nutaton angle	Reynolds	magnetic Reynolds	aspect ratio	precession ratio
$f_c = \frac{\Omega_c}{2\pi}$	$f_p = \frac{\Omega_p}{2\pi}$	α	$Re = \frac{\Omega_c R^2}{\nu}$	$Rm = \frac{\Omega_c R^2}{\eta}$	$\Gamma = \frac{H}{R}$	$Po = \frac{\Omega_p}{\Omega_c}$
0...10 Hz	0...1 Hz	$45^\circ \dots 90^\circ$	up to 10^8	up to 700	2	0...0.1

- natural forcing allows efficient flow driving without propellers or pumps
- Gans' experiments in the 70's yield field amplification by a factor of 3
- precession dynamos are found in simulations around $Rm \sim O(10^3)$

Inertial waves & amplitudes

Quantitative analysis by decomposing u_z in axial modes $\propto \sin(\pi z k/H)$ with axial wavenumber k and Fourier transformation in azimuth and time

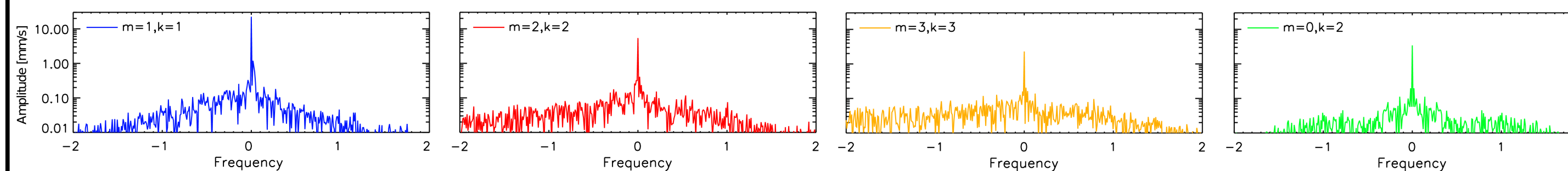


Fig. 3: Spectra of the directly forced mode (blue), its first harmonics (red & orange) and the axisymmetric flow (green) from simulations in the precession frame with $Re=10^4$ and $Po=0.10$.

- laminar flow consisting of large scale inertial modes (standing waves in precession frame) with only weak time-dependent contributions

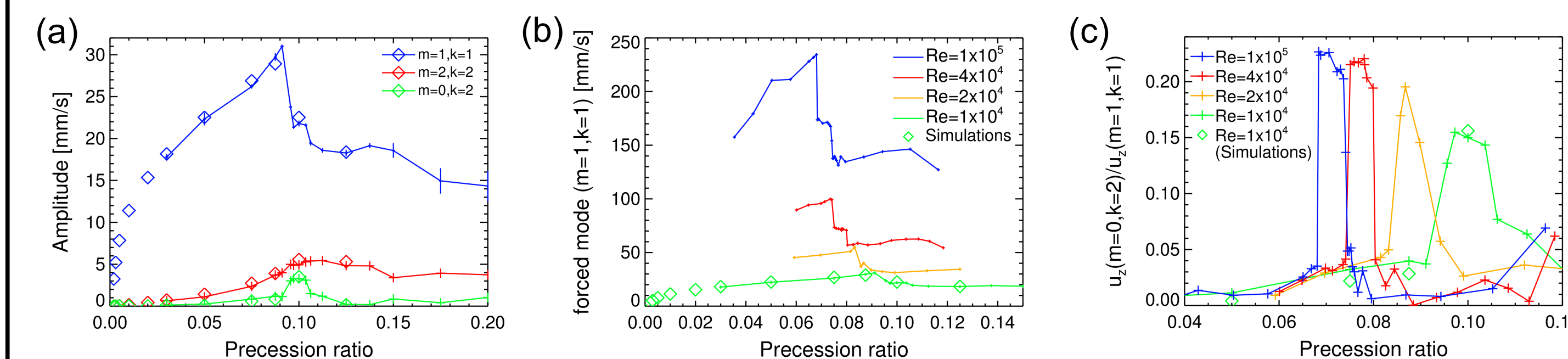


Fig. 4: (a) Amplitude of dominant modes for $Re=10^4$ and $Po=0.1$. (b) Amplitude of forced mode $(m,k)=(1,1)$ for various Re . (c) Relative amplitude of the axisymmetric mode $(m,k)=(0,2)$ for various Re . The width of the regime with axisymmetric mode (~ 0.006) is rather independent of Re .

- resonance-like emergence of axisymmetric mode in conjunction with reduction of amplitude of directly forced mode $(m,k)=(1,1)$

Structure of axisymmetric mode

- double roll structure in the meridional plane (similar to mean flow in VKS)
- geostrophic azimuthal mode opposite to solid body rotation

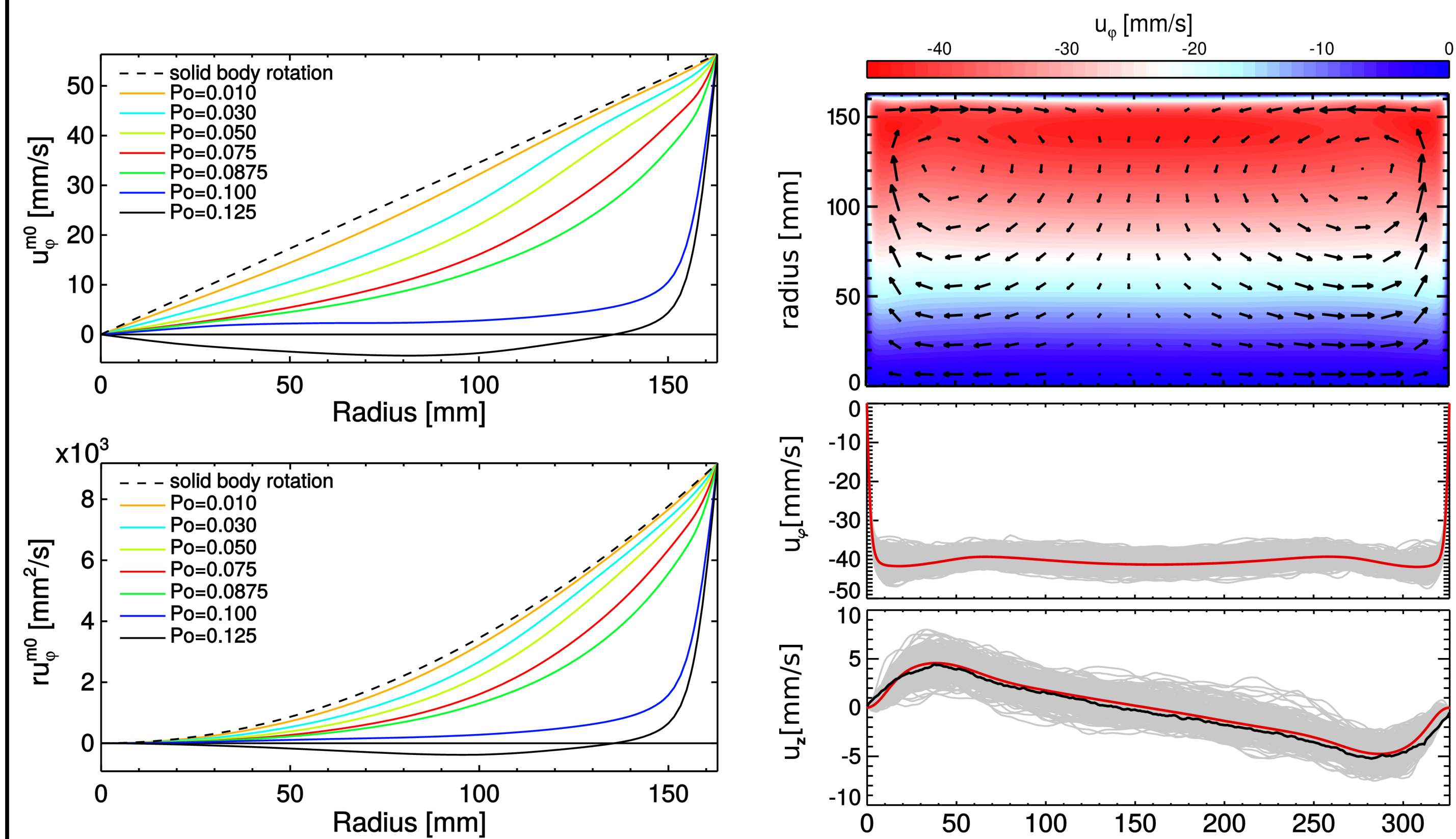


Fig. 5: Radial profiles of the time-averaged azimuthal velocity (top) and the corresponding angular momentum (bottom) in the equatorial plane from simulations at $Re=10^4$. The Rayleigh criteria is violated when the slope of ru_ϕ becomes negative.

- strong axisymmetric mode within narrow regime of precession ratios
- goes along with suppression of solid body rotation
- violation of Rayleigh's instability criteria for rotating flows $\frac{d}{dr}(u_\phi r) < 0$

Kinematic dynamos

The time-averaged velocity fields obtained from hydrodynamic simulations constitute the basis for kinematic dynamo models. The magnetic induction equation is solved numerically using pseudo-vacuum boundary conditions.

$$\frac{\partial}{\partial t} \mathbf{B} = \nabla \times (\mathbf{u} \times \mathbf{B} - \eta \nabla \times \mathbf{B})$$

- results show dynamo action at $Rm_{crit} = 430$ when applying the flow field from $Re=10^4$ and $Po = 0.1$
- essential for the dynamo is the combination of axisymmetric flow ($m=0$) and the directly forced mode ($m=1$)
- flow fields obtained at other values of Po exhibit dynamo action only around $Rm_{crit} \approx 2000 \dots 5000$ (far above values achievable in the planned experiment)

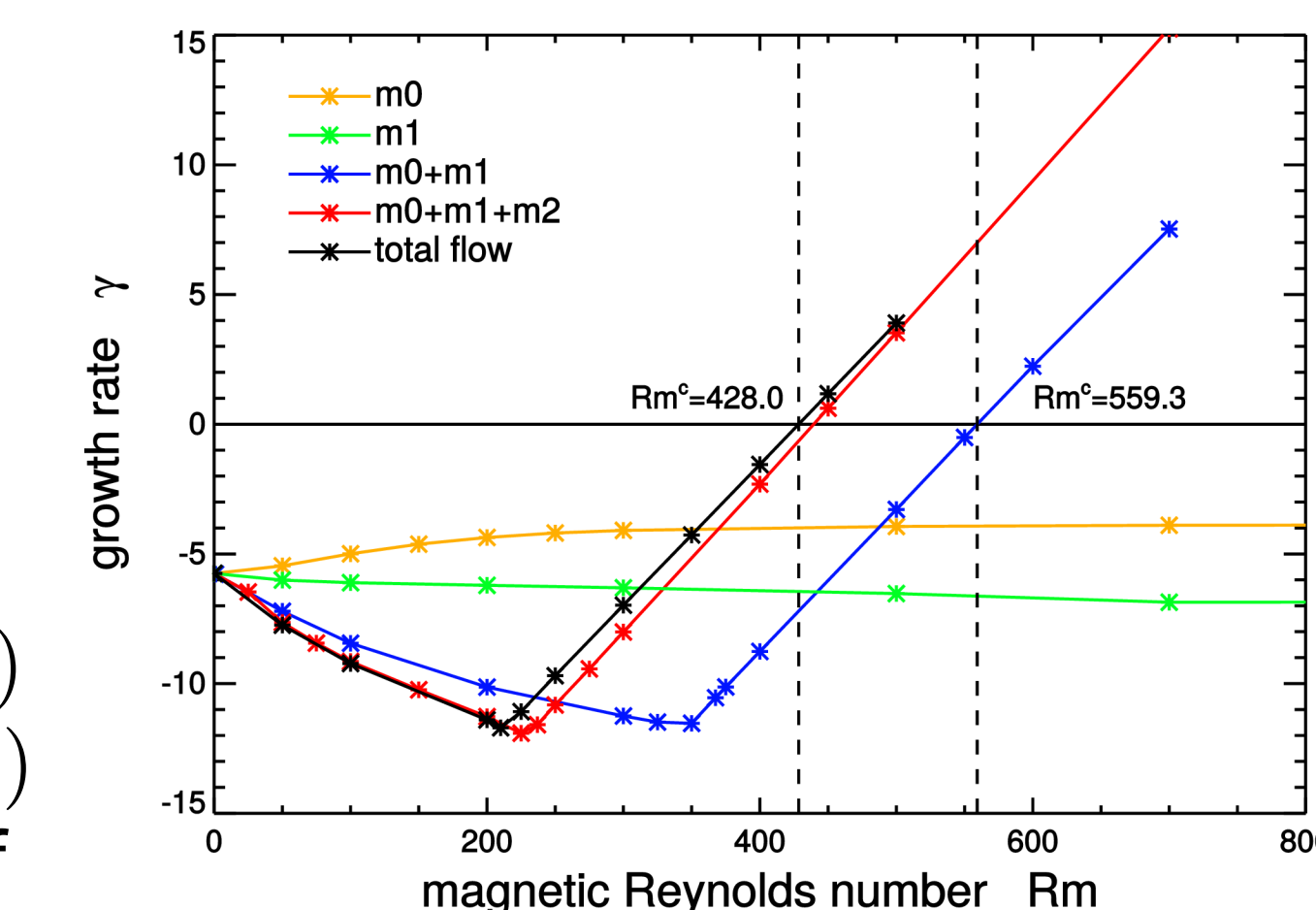


Fig. 7: Growth rates vs Rm for combinations of various azimuthal velocity modes obtained from simulations at $Re=10^4$ and $Po=0.1$

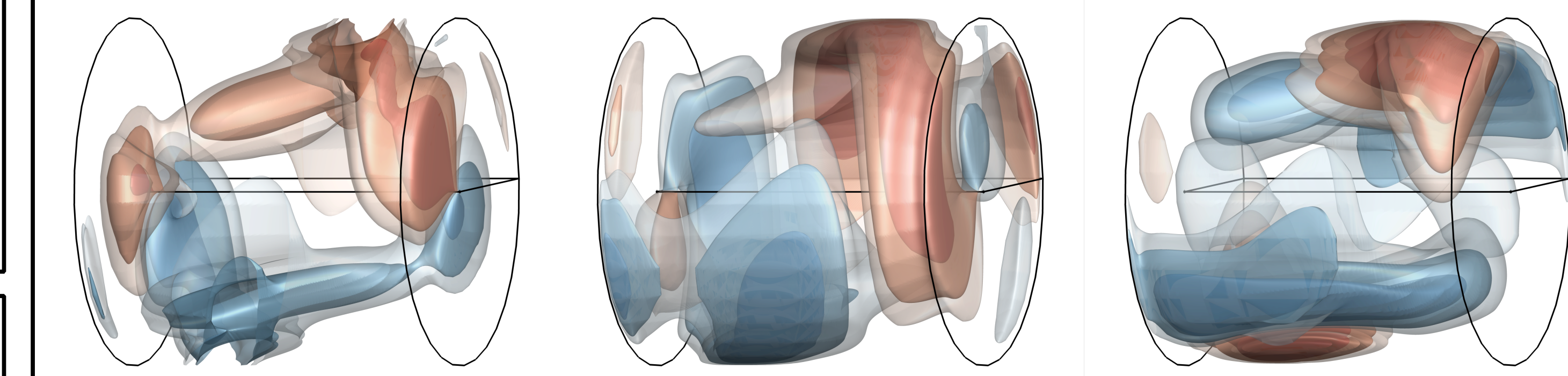


Fig. 8: Structure of the magnetic field at 12.5, 25, 50% of its maximum value. From left to right: B_r, B_ϕ, B_z . The field structure propagates around the cylinder axis.

Conclusions for the planned sodium dynamo

Dynamos possible at Rm achievable in the planned experiment in a narrow regime characterized by presence of an axisymmetric mode

Scaling to planned sodium experiment:

- emergence of $m=0$ mode is connected with hysteresis found for transition into turbulent flow state at larger Re
- occurs at smaller Po when Re is increased
- measurements of power consumption and pressure point out asymptotic behavior with $Po_{crit} \approx 0.06 \dots 0.07$ for $Re \geq 10^6$

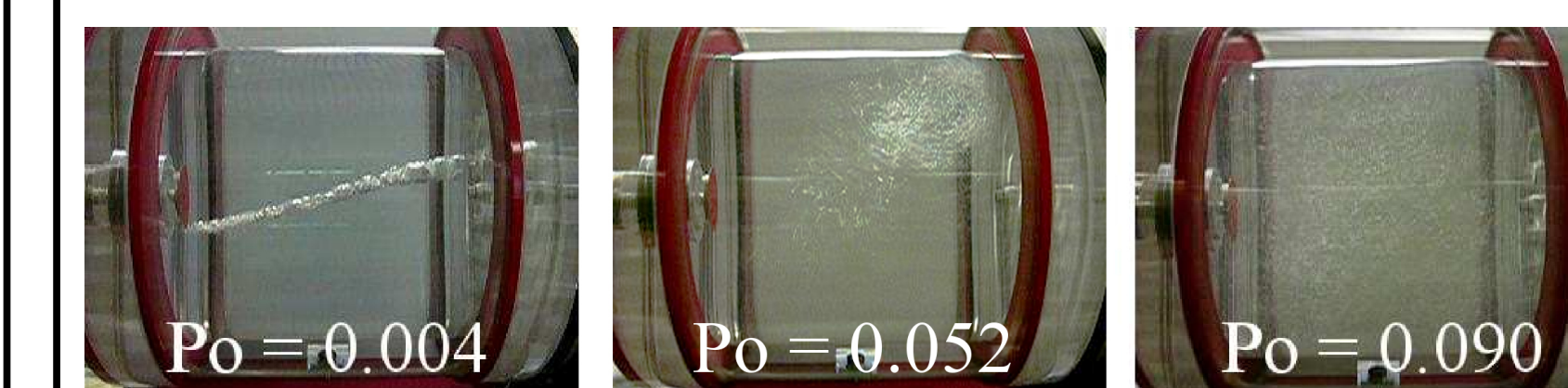


Fig. 9: Jump in electrical power consumption and hysteresis at transition to turbulent state. Experiment $Re=10^6$

- $Rm_{crit} \approx 430$ corresponds to $f_c \approx 5 \dots 6$ Hz
- $Po_{crit} \approx 0.06$ corresponds to $f_p \approx 0.35$ Hz
- global quantities (pressure, motor power, torque) for characterisation of flow state

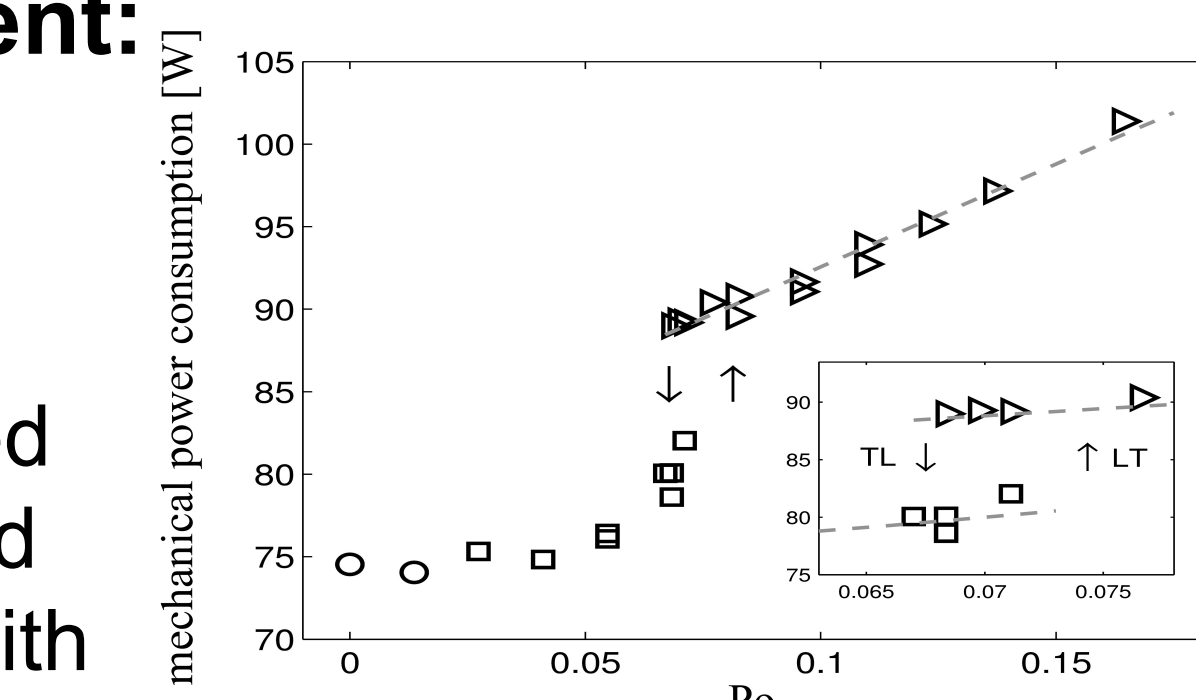


Fig. 10: Transition from laminar state (left) to a nonlinear fluid behavior (center) finally resulting in a turbulent flow above a critical precession ratio (right). $Re=2 \times 10^6$

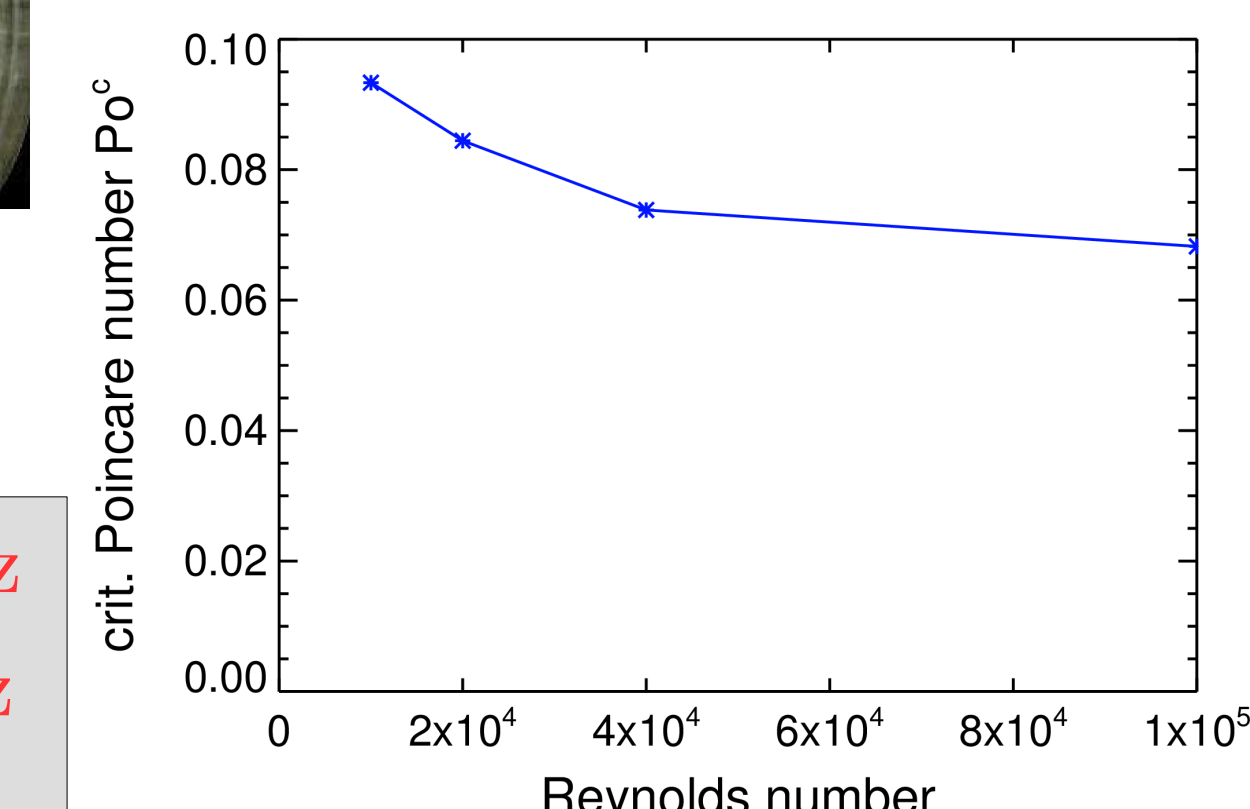


Fig. 11: Critical Po for appearance of axisymmetric mode from experiment

see Giesecke et al., arxiv: 1708.06314

Hydrodynamic simulations & experiments

We conduct numerical simulations with SEMTEX (Spectral Element-Fourier method) and flow measurements in a down-scaled water experiment with Ultrasonic Doppler Velocimetry (UDV) (Fig. 2a)

$$\frac{\partial}{\partial t} \mathbf{u} + \mathbf{u} \cdot \nabla \mathbf{u} = -\nabla P - 2\Omega_p \times \mathbf{u} + \nu \nabla^2 \mathbf{u} \text{ and } \mathbf{u}_{bc} = \Omega_c \times \mathbf{r}$$

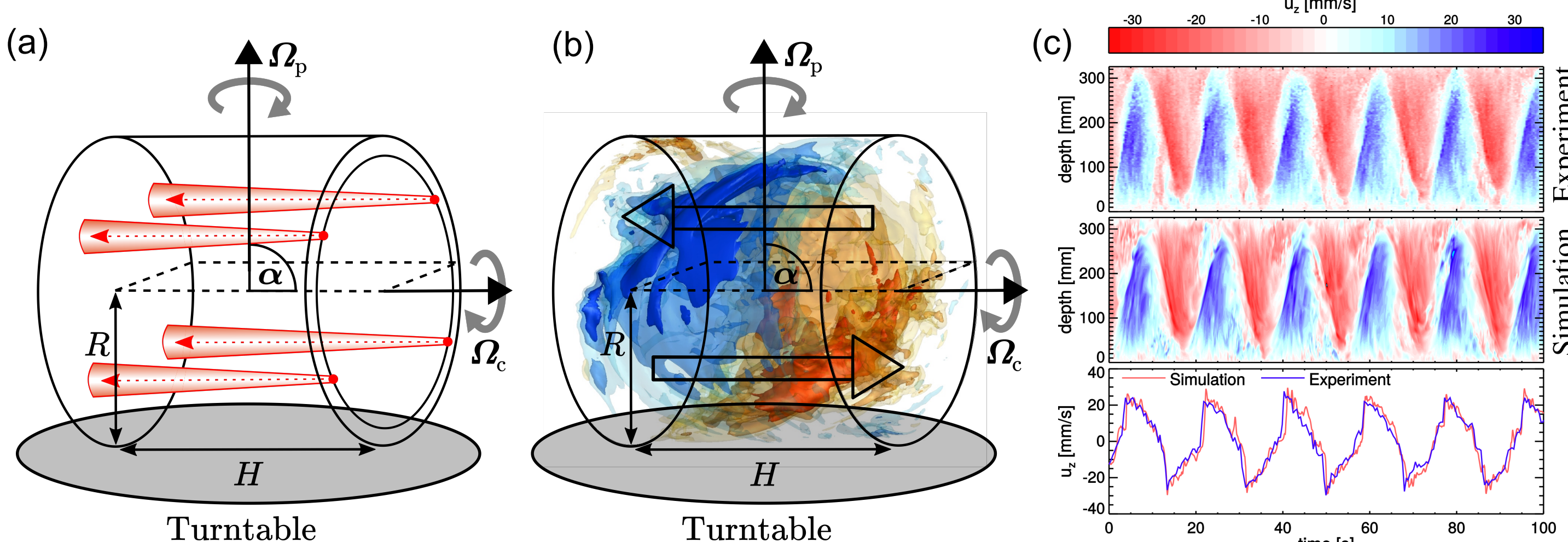


Fig. 2: (a) Set-up of the experiment with location of UDV probes. Nutation angle is fixed at $\alpha = 90^\circ$. (b) Iso-surfaces of axial velocity from simulations that illustrate the recirculation flow (arrows), the concentration in the vicinity of the lateral walls, and the tilt with respect to the symmetry axis. (c) Direct comparison of UDV measurements (top) and simulations (center) at $Re=10^4$ and $Po=0.10$

- excellent agreement between simulation and experiment at $Re=10^4$ which is the upper limit for simulations and lower limit for motor (Fig. 2c)
- flow determined by directly forced flow ($m=1$) overlapped by higher azimuthal modes (essentially $m=2$) that represent standing inertial waves due to nonlinear self-interactions (Fig. 2b and 2c)